Mon. Not. R. Astron. Soc. **372,** 60–68 (2006) doi:10.1111/j.1365-2966.2006.10745.x

New evidence for a linear colour–magnitude relation and a single Schechter function for red galaxies in a nearby cluster of galaxies down to $M^* + 8$

S. Andreon,[1⋆] J.-C. Cuillandre,[2,3] E. Puddu[4] and Y. Mellier[5]

[1]*INAF–Osservatorio Astronomico di Brera, via Brera 28, 20121 Milano, Italy*
[2]*Canada–France–Hawaii Telescope, PO Box 1597, Kamuela, HI, 96743, USA*
[3]*Observatoire de Paris, avenue de L'Observatoire 61, 75014 Paris, France*
[4]*INAF–Osservatorio Astronomico di Capodimonte, Salita Moiariello, 16 80131 Napoli, Italy*
[5]*CNRS UMR 7095, Institut d'Astrophysique de Paris, bd Arago 98bis, 75014 Paris, France*

Accepted 2006 June 27. Received 2006 June 20; in original form 2006 April 6

ABSTRACT

The colour and luminosity distributions of red galaxies in the cluster Abell 1185 ($z = 0.0325$) were studied down to $M^* + 8$ in the B, V and R bands. The colour–magnitude (CM) relation is linear without evidence for significant bending down to absolute magnitudes that are seldom probed in the literature ($M_R = -12.5$ mag). The CM relation is thin (± 0.04 mag) and its thickness is quite independent of the magnitude. The luminosity function (LF) of red galaxies in Abell 1185 is adequately described by a Schechter function, with a characteristic magnitude and a faint end slope that also well describe the LF of red galaxies in other clusters. There is no passband dependence of the LF shape other than an obvious M^* shift due to the colour of the considered population. Finally, we conclude that, based on colours and luminosity, red galaxies form a homogeneous population over four decades in stellar mass, providing a second piece of evidence against faint red galaxies being a recent cluster population.

Key words: methods: statistical – galaxies: clusters: general – galaxies: clusters: individual: Abell 1185 – galaxies: evolution – galaxies: fundamental parameters – galaxies: luminosity function, mass function.

1 INTRODUCTION

One of the major problems facing models of galaxy formation is why cold dark matter models predict a larger number of low-mass galaxies than observed. Today, extremely faint ($M \gg M^* + 5$ mag) galaxies are still a poorly studied population because they are difficult to find and, once found, the measurement of their properties is not trivial since the measured properties are usually strongly affected by selection effects. Thus, understanding the properties of the lowest luminosity galaxies, which are presumably also very low mass, might shed light on some of the unsolved questions related to the production of galaxies in low-mass halos.

The bulk of the observational work on low-luminosity galaxies is limited to the environment of clusters. The pioneering work by Visvanathan & Sandage (1977) presents the colour–magnitude (CM) relation over an 8-mag range, although the very large majority of the data is relevant to the brightest 4 mag. Secker, Harris & Plummer (1997) reports that the CM relation (also known as the red sequence) is linear in the Coma cluster over a 7-mag range, i.e. down to $M_R = -15.0$ mag. Conselice, Gallagher & Wyse (2002) confirms that galaxies in the first 4 mag of the Perseus clusters obey the usual CM relation (e.g. Bower, Lucey & Ellis 1992), but faint candidate members of the cluster tend to depart from the colour of the red sequence, being bluer or redder. The scatter around the red sequence is small ($\sigma \approx 0.07$ mag) down to $M_R \sim -17$ mag, but rises to $\sigma \approx 0.5$ mag at $M_R \sim -14$ mag. Instead, Evans, Davies & Phillipps (1990) found that the fainter Fornax galaxies become redder, not bluer. Therefore, it is unclear what the shape of the red sequence at faint magnitudes is, and if it is universal or if it changes from cluster to cluster.

In other environments, information is even scarcer. In the review article by Mateo (1998) on dwarf galaxies in the Local Group, the CM relation includes about 30 galaxies in the range $-22 < V < -11$ mag. Blanton et al. (2005) derived luminosity and colour distributions of faint galaxies in the local Universe for a flux and surface brightness limited sample. However, it is unclear how much their results are affected by the fact that they assume no environment dependence and a uniform spatial distribution of the studied sample and that, later on, the distributions were claimed environmental-dependent and the sample clustered (see Andreon, Punzi & Grado 2005, hereafter APG, for a discussion).

⋆Email: andreon@brera.mi.astro.it

In this paper, we report results about a volume complete sample of galaxies in a nearby cluster of galaxy, Abell 1185. Our data are deep enough to reveal extremely faint objects, allowing us to investigate the properties of red galaxies over a 9-mag range.

Abell 1185, a cluster having richness 1 (Abell 1958), has a redshift of $cz = 9800\,\mathrm{km\,s^{-1}}$ and a velocity dispersion of $\sigma_v = 740 \pm 60\,\mathrm{km\,s^{-1}}$ (Mahdavi et al. 1996), and an X-ray luminosity of $L_X(0.5\text{–}3\,\mathrm{keV}) = 1.6\,10^{43}\,h_{50}^{-1}\,\mathrm{erg\,s^{-1}}$ (Jones & Forman 1984).

For the Abell 1185 cluster, we adopt a distance modulus of 35.7 mag ($H_0 = 70\,\mathrm{km\,s^{-1}\,Mpc^{-1}}, z = 0.0325$).

2 THE DATA AND DATA REDUCTION

Abell 1185 observations and data reduction follow closely a similar analysis performed on the Coma clusters (Andreon & Cuillandre 2002, AC02 hereafter), to which we defer for details.

B, V and R cluster observations were taken on 2003 January 31 in photometric conditions, with the CFH12K camera (Cuillandre et al. 2000) at the Canada–France–Hawaii Telescope (CFHT) prime focus in photometric conditions. CFH12K is a 12 288 × 8192 pixel CCD mosaic camera, with a $42 \times 28\,\mathrm{arcmin^2}$ field of view and a pixel size of 0.206 arcsec. Five dithered images per filter were taken, pre-reduced (overscanned, biased, darkened and flat-fielded) and then optimally stacked. The total exposure time was 1500, 1200 and 900 s in B, V and R, respectively. Seeing in the combined images is 1.2 to 1.3 arcsec FWHM. The CFHT CCD mosaic data reduction package FLIPS (Magnier & Cuillandre 2004) was used. After discarding areas noisier than average (gaps between CCDs, borders, regions near bright stars, etc.), the usable area is $0.263\,\mathrm{deg^2}$, or $1.3\,\mathrm{Mpc^2}$ at the cluster redshift. Images were calibrated in the Bessel–Cousin–Landolt system through the observation of photometric standard star fields listed in Landolt (1992).

Fig. 1 shows a highly compressed R-band image of Abell 1185.

In this work, interloper galaxies are statistically removed. This requires that the cluster and the control field images share the same photometric system: in the presence of colour mismatches, which often arise from using data coming from different telescopes/instruments/filters, the background contribution is usually assumed to be perfectly removed, whereas instead it leaves some residuals, biasing the luminosity function (LF) and colour measurements. Our control field has been published and described in McCracken et al. (2003). These images were taken using the very same B, V and R filters, telescope and instrument used for the present study; they were reduced by the same software, calibrated in the same photometric system by the same standard fields, hence assuring a perfect homogeneity between the two data sets. The control field is much deeper than the cluster observations and therefore we consider only the magnitude range that matches the cluster images. Even if our data are homogeneous, we nevertheless verified that cluster and control field images share the same locus of stars, in the $V - R$ versus $B - V$ colours (e.g. as in fig. 1 of Andreon, Lobo & Iovino 2004) and in the $(V - R) - (B - V)$ versus $B - V$, in order to enhance the visibility of any mismatch. As a further check, we compared the density distribution of galaxies in the $V - R$ versus $B - V$ plane, and did not detect any colour offsets between the cluster and the control field images.

Objects are detected using SExtractor (Bertin & Arnouts 1996), using an isophotal threshold of 26.0, 25.5 and 24.5 in B, V and R, respectively, corresponding to a threshold of $\approx 2\sigma$ of the sky in the cluster images and more than 5 σ in the control field images.

In this paper, we adopt SExtractor isophotal corrected magnitudes as a proxy for 'total' magnitudes; we do not choose Kron magnitudes because of their flip-flopping nature described in APG. Completeness is measured as the magnitude of the brightest low surface brightness galaxy of the faintest detectable central surface brightness, as described in Garilli, Maccagni & Andreon (1999). Cluster data are complete down to $B = 24.0, V = 23.8$ and $R = 22.7$ mag, but are further clipped to a brighter magnitude range ($B = 23.25$ or $V = 22.45$ or $R = 22.0$ mag, depending on the measured quantity), in order to be nearly 100 per cent complete in colour and in order to reduce the Eddington bias (see section 3.5.2 in AC02 for details). Fundamentally, from more than 10 000–20 000 detections

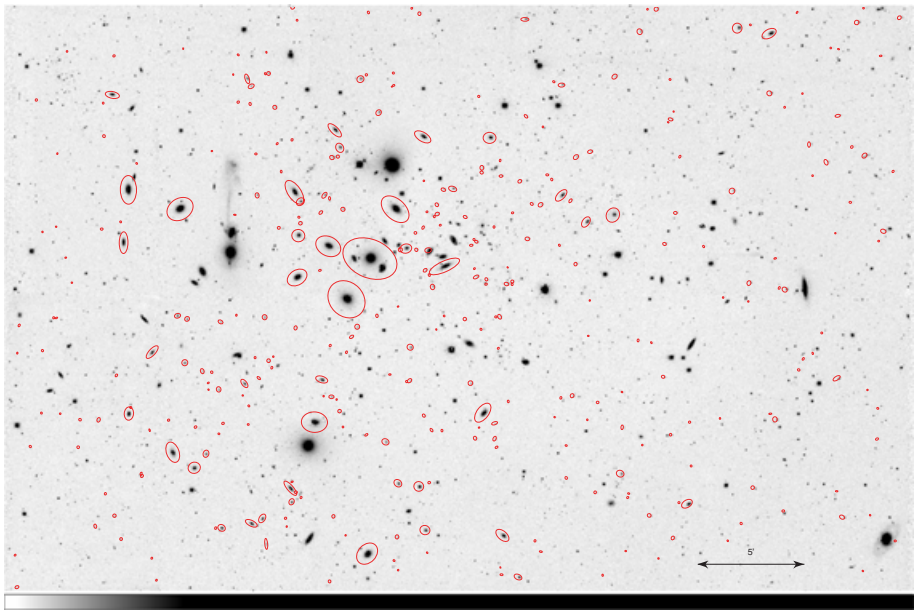

Figure 1. The (compressed) image of the studied field in the R band, with about 400 red galaxies (members and background) marked with an ellipse. North is up and east is to the left. The field of view is $42 \times 28\,\mathrm{arcmin^2}$.

in the cluster line of sight, we select the brightest 2000 galaxies with the rationale of keeping the best data.

Stars are discarded by combining the probabilities derived by SExtractor in the three filters. We conservatively keep a high threshold, rejecting 'sure stars' only ($class_{\rm star} > 0.95$) in order not to exclude the compact galaxies, while leaving some residual stellar contamination in the sample: it (as well as the contamination caused by background galaxies) is dealt with statistically later on. Most galaxies are easily classified as extended sources in the magnitude range of our interest. Very compact galaxies, such as NGC 4486B or M32, are however easily misclassified as stars at the distances of the Fornax (Drinkwater et al. 1999) and Coma (AC02) clusters, but they represent a minority population (Drinkwater et al. 1999, AC02). Finally, blends of globular clusters (GCs) that are not resolved in individual components due to seeing and that look like dwarf galaxies on our ground-based images are expected, but from what is observed in the Coma cluster (AC02), the GC blends start to contaminate galaxy counts at fainter magnitudes than the range probed in this work.

3 RESULTS

3.1 Exploring the colour–colour–magnitude data cube

Let us explore the colour–colour–magnitude cube by observing it through different projections.

Fig. 2 is a projection of the colour–colour–magnitude cube that aligns the observer's eye along the CM relation. The projection is along an axis slightly tilted with magnitude, with slopes 0.2/6 and 0.1/6 mag in $B-V$ and $V-R$, respectively (these are logically the slopes of the CM relations in the two colours). Technical details about the way the CM slope is determined are given in the Appendix. Colours are corrected to $R = 20$ mag for the slope of CM. The left and right panels refer to galaxies in the cluster and in the control field lines of sight, respectively. The number density distribution of control field galaxies (right panel) shows a shallow gradient from bottom-right to top-left, more evident when the whole control field data set is plotted (in the figure, only one galaxy out of 4.7 is plotted to account for differences in the surveyed area and to make the two panels easy to compare by eye). Superimposed onto the shallow gradient, the colour distribution of galaxies in the cluster line of sight (left panel) shows a clear excess at $B-V = 0.98, V-R = 0.62$ mag, marked with a circle in the figure.

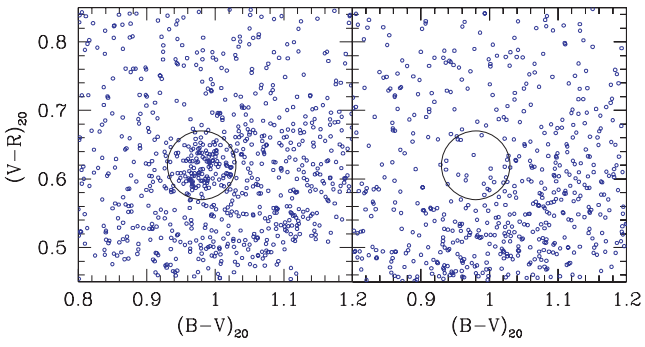

Figure 2. Colour–colour distribution of galaxies in the cluster (left panel) and control field (right panel) lines of sight. An obvious overdensity is seen at the colour of the red sequence ($B-V = 0.98, V-R = 0.62$ mag). Colours are corrected to $R = 20$ mag for the CM effect. In the right panel, we randomly plot 1 out of 4.7 galaxies from the control field galaxies, in order to account for differences in surveyed areas.

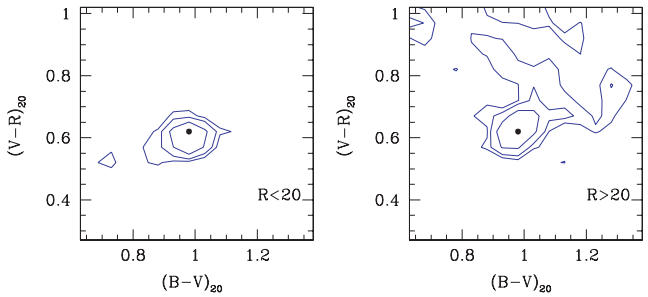

Figure 3. Background subtracted number density distribution of Abell 1185 members in the colour–colour plane. The left and right panels show the distribution of $R < 20$ mag ($M_R = -15.7$ mag) and $R > 20$ mag, respectively. Contours are draw to levels set at 1/2, 1/4 and 1/8 of the peak value. The extension in the right panel towards red colours of the lowest contour has an $S/N \sim 1$.

Fig. 3 shows the colour distribution, binned in colour bins and background subtracted using our control field. The direction that points to the observer is now the number density of Abell 1185 members of a given colour. The two panels display the result for galaxies brighter (left panel) and fainter (right panel) than $R = 20$ mag ($M_R = -15.7$ mag). A clear peak at the colour of the CM relation is seen in both panels. The peaks are narrow: they have a width of ± 0.04 mag (see Appendix), implying that the thickness of the red sequence is small. In Fig. 3, the shown distributions are the observed distributions convolved by a 0.1-mag top-hat kernel. The two peaks are almost centred at the same colour ($B-V = 0.98, V-R = 0.62$ mag), shown as points in the figure. In the left panel, there is an insignificant 0.02-mag offset in $V-R$, 1/5 of the width of the colour bin. This implies that the CM relation does not deviate from linearity at faint magnitudes. A 0.1-mag shift would be very easily identified in the above plot.

Fig. 3 also shows that Abell 1185 has a low fraction of blue galaxies in the observed portion (our images sample about half of the cluster virial radius, which was computed from the cluster velocity dispersion using equation 1 of Andreon et al. 2006): the peak does not show any large extension towards bluer (say, 0.2 mag or more) colours. The signal-to-noise ratio (S/N) of the top-right part of lowest contours in the right panel of Fig. 3 is $\sim$1. Therefore, the extension towards red colours of the $R > 20$ distribution is hardly significant at all.

Fig. 4 shows the distribution of galaxies in the CM plane of galaxies in the Abell 1185 line of sight. Each panel shows galaxies falling in a plane of the colour–colour–magnitude cube of thickness 0.4 mag in the other colour, in order to reduce the contamination by background galaxies. Because the spread around the red sequence is 5 times smaller (see Fig. 3 and Appendix), the $0.4\,(+\,-\,0.2)$ mag thickness is wide enough to avoid selectively removing any red sequence galaxy and therefore does not bias the slope of the red sequence. After the above selection, we know from control field data that only one in five of the plotted galaxies is a cluster member. The CM relations in $B-V$ and $V-R$ versus R are outstanding for galaxies brighter than $R = 20$ or 21 mag. At fainter magnitudes, the background contribution makes the CM relation difficult to disentangle. However, Fig. 3 shows that, at $R > 20$, the CM relation does not bend.

Fig. 5 shows the number density distribution in the CM plane after background subtraction. In order to reduce the noise due to background fluctuations, we considered only galaxies within ± 0.1 mag in $V-R$ from the red sequence, which is a sensible choice given the small $V-R$ scatter of red galaxies. As in Figs 2 and 3, we have

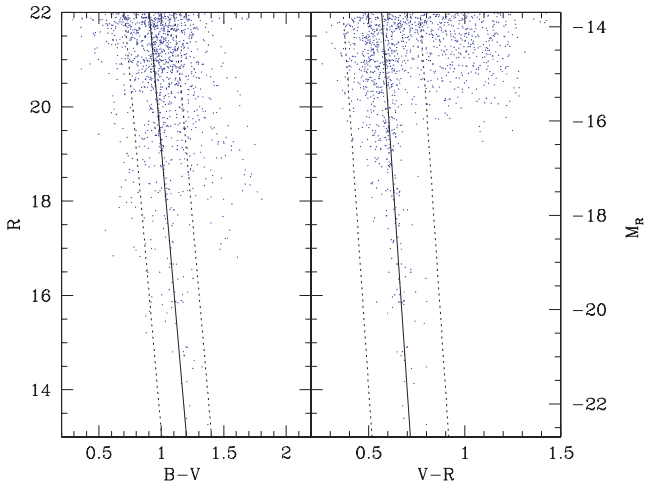

Figure 4. Colour–magnitude distribution of galaxies in the Abell 1185 line of sight. Each panel contains plots of galaxies within 0.2 mag from the red sequence in the other colour. Based on the control field images, we estimate that only one in five of the plotted galaxies is a cluster member.

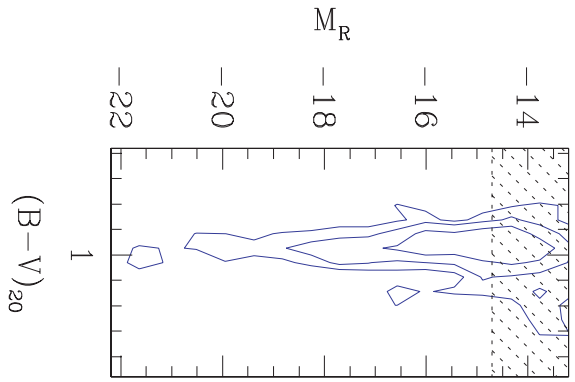

Figure 5. Background subtracted number density distribution of Abell 1185 members in the colour–magnitude plane. Each panel shows galaxies falling in a plane of the colour–colour–magnitude cube of thickness 0.4 mag in the other colour, in order to reduce the contamination by background galaxies.

magnitude-corrected colours to align the R magnitude with one of the figure axis. As in Fig. 3, the data are convolved (binned) by a top-hat function of ±0.05-mag width in colour. The shaded region is subject to borders effects. The figure confirms the linearity of the red sequence and its almost constant width.

The interpretation of these results is deferred to Section 4.4.

We define as red galaxies the objects having colours within 0.1 mag from both CM relations. Such a definition leaves intact the peak of the colour distribution centred on red galaxies (see in particular Fig. 3) and leaves room for objects scattered off from the red sequence by (our small) photometric colours.

The sample of red galaxies turns out to be composed of about 180 members plus a similar number of background galaxies. As a further check, we consider a second sample, relaxing the tightness of the colour constraint from 0.1 to 0.2 mag. The number of red galaxies remains unchanged, but the number of background galaxies grows by more than a factor 4!

3.2 The luminosity function

3.2.1 Methods

Two methods are used to perform the statistical subtraction. For display purposes, we use the traditional method, put forward by, say, Zwicky (1957) and Oemler (1974), and summarized in many recent papers. The cluster luminosity function is computed as the difference between galaxy counts in the cluster and the control field directions, after binning the events (galaxy magnitudes) in magnitude bins. Approximate errors are computed as the square root of the variance of the minuend, because the contribution due to the uncertainty on the true value of background counts is negligible. Secondly, we fit the unbinned galaxy counts without any use of binned data or errors computed in the previous approach. At this point, we follow the rigorous method set forth in APG, which is an extension of Sandage, Tammann & Yahil (1979, STY) to the case where a background population is present. The custom method adopts the extended likelihood instead of the conditional likelihood used by STY. The method (fully described in APG) consists of fitting the unbinned distribution of clusters and control field counts using the likelihood and of computing confidence intervals using the likelihood ratio theorem (Wilks 1938, 1963). The advantage of the rigorous method is that it provides unbiased results and reliable errors estimations, hence assuring the correctness of the result.

3.2.2 The LF of red galaxies

Fig. 6 shows the resulting LFs of red galaxies in the three filters: the binned data with approximated error bars, and the best-fitting Schechter (1976) function with its uncertainty. Bins with incomplete data coverage are not plotted. The best-fitting parameters and their errors are listed in Table 1. This table also provides the range adopted for the fitting, a range such that the LF is unaffected by the $R <$ 22.00 mag initial selection.

In Fig. 7, 68 per cent confidence contours are shown. The m^* (or m^*) values, once values at the same slope α are considered, differ by the colour of red sequence galaxies. The α values in different bands are almost identical. This is expected, because no passband dependence of the red galaxies LF is possible as long as the CM relation is linear. In fact, linear mapping (R to B or V, in order to account for the CM relation) has a constant Jacobian and cannot alter the shape of a distribution function. The detection of a passband dependence for a sample selected to obey to a linear CM relation is instead a sign of problems in the data analysis.

The slope of the LF is determined with good accuracy (±0.06) in all three bands but the uncertainty on the characteristic magnitude is large (≈0.6 mag), because we are studying a single, not so rich cluster. We find that there are only about 20 red galaxies between m_3 and $m_3 + 2$ inside the studied portion of Abell 1185.

The best-fitting parameters are robust to the adopted width of the colour selection. Using a ±0.2-mag width in place of our reference ±0.1-mag width, we find in R: $m^* = 13.9 \pm 0.5$ and $\alpha = -1.18 \pm 0.09$, in good agreement with the best-fitting parameters found by adopting a more stringent colour cut. Furthermore, 16 out of the 18 data points computed with the two colour selections differ from each other by less than half the error bar in a non-systematic way, clarifying that our reference colour boundary does not bias the LF. In particular, the above comparison shows that the Eddington bias is negligible, as expected.

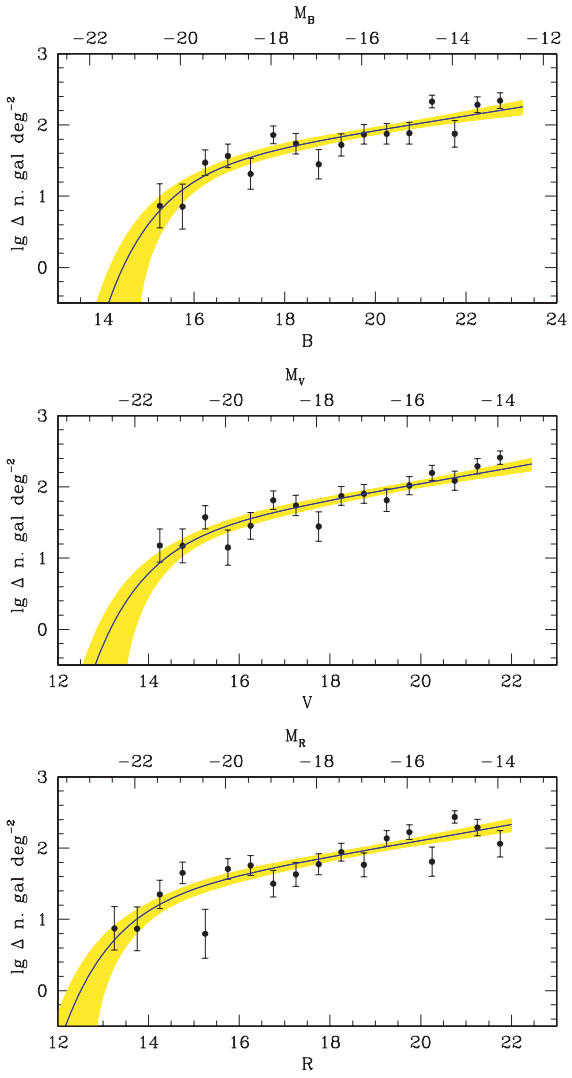

Figure 6. *B*-, *V*- and *R*-band LF of red galaxies in Abell 1185. Data points and error bars are derived by binning the data in magnitude bins (and using an approximate error computation), whereas the curve traces the best-fitting LF of unbinned data and the shaded area marks the model uncertainty.

Table 1. Fit results.

Filter	Range	m^*	α
B	$B < 23.25$	15.7 ± 0.5	-1.25 ± 0.06
V	$V < 22.45$	14.3 ± 0.5	-1.28 ± 0.06
R	$R < 22.00$	13.7 ± 0.7	-1.28 ± 0.06

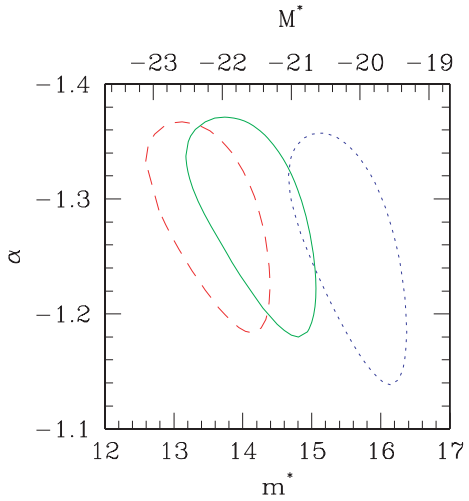

Figure 7. B, V and R (from right to left) 68 per cent confidence contours ($2\Delta \ln \mathcal{L} = 2.30$) on m^* (M^* in the top x-axis) and α.

4 COMPARISON AND DISCUSSION

4.1 Comparison with the red sequences from other clusters

The red sequence of Abell 1185 has none of the specific features that is attributed to other clusters/environments by other works. The red sequence is linear and does not bend towards the blue at faint magnitudes, as Conselice et al. (2002) found for candidate members of the Perseus cluster. It neither bends towards the red as Evans et al. (1990) found for Fornax galaxies. The small scatter at faint magnitudes is much smaller than the 0.5-mag scatter that Conselice et al. (2002) found for candidate members of the Perseus cluster. Simply put in a few words, extremely faint galaxies in Abell 1185 follow the extrapolation of brighter red galaxies.

We underline that each of these features we do not detect may be reproduced by mismatches between cluster and control field images or by an incorrect estimation of the galaxy membership. On the other hand, it is highly unlikely that these effects would render linear an intrinsically bent red sequence, or would strongly reduce the scatter of a scattered red sequence.

Our claim of a linear CM of Abell 1158 is in apparent disagreement with the Ferrarese et al. (2006) claim of a non-linear CM in Virgo. In order to cross check their results, we take advantage of the fact that the authors generously shared their data. We consider two models: a linear and a quadratic CM relation, as considered by the authors. We assume normal errors on colours and an intrinsic scatter, and we compute the likelihood following the laws of probability (the likelihood for this problem is presented in D'Agostini 2005 and in the appendix of Andreon 2006). Computation of evidence (e.g. Liddle 2004, for an astronomical introduction) and information content (e.g. Trotta 2005) clarify that either data are non-informative or, if any, they support the simpler model (a linear CM) and surely do not support the extended model (i.e. the quadratic CM). We note that while Ferrarese et al. (2006) acknowledge the existence of an intrinsic scatter, they do not account for it in the error computation (while it is accounted for in the present statistical analysis). Ignoring this component makes their fit to the bright and faint halves of their sample incompatible with each other, while they become compatible once the intrinsic scatter is accounted for.

Our data, by contrast, are informative because they allow us to differentiate between a linear and non-linear model. Furthermore, we do not need any complex statistical analysis to differentiate them because of our small errors. Any potential 0.05-mag CM drift away from the linear CM is equal to the total observed (intrinsic plus photometric) scatter around the CM in Abell 1185. For Virgo, it is one-third of the observed scatter. In case of Abell 1185, a 0.1-mag drift is easily spotted even by eye (for example in Fig. 3), whereas in case of Virgo it requires an advanced statistical analysis that ought to conclude that the data are largely uninformative about the CM curvature.

We emphasize that there is no colour selection in Fig. 3, and therefore we do not miss the possible CM bending (curvature) because of selection effects. A 0.05-mag drift away from a linear CM would lead to a distribution having different centres in the two panels by 0.05 mag, which is ruled out. In Fig. 4, the colour selection (± 0.2 mag) is wider than a possible 0.05-mag drift and the CM does not become linear because its bending part is cut away by the colour selection.

4.2 Comparison with the literature LFs of red galaxies

Fig. 8 shows our V-band LF and its uncertainty (shaded region) and some literature LFs of red galaxies. All LFs have been normalized to the richness (computed for galaxies brighter than $M_V = -18$ mag) of Abell 1185. Secker & Harris (1996) compute the LF of the Coma cluster in the R band, converted to V using the observed $V - R$ colour of Abell 1185 red galaxies. Smail et al. (1998) compute the I-band LF of red galaxies in some clusters at $z \sim 0.25$, well matching V-band observations in the cluster frame. In order to plot their data on Fig. 8, we only need to compute the (small, 0.1 mag) $E + K$ correction, derived using Bruzual & Charlot (1993), and the distance modulus of the studied clusters. These authors provide two red LFs, one based on the use of a homogeneous cluster and control field, plotted in Fig. 8, and a second one using heterogeneous data (which are not considered here for the present comparison, in light of the mentioned difficulties in using heterogeneous data for LF studies). The red galaxy LF of Abell 1185 matches well these red galaxy LFs. Of course, every work adopts a slightly different definition of 'red galaxy', such as using a different width around the CM (e.g. the Secker & Harris 1996 choice is twice as large as ours), or increasing it with magnitude to account for a larger photometric scatter at fainter magnitudes (e.g. Smail et al. 1998), or using different filters (in both the observer and cluster frames). The current agreement of these LFs shows that the LF is robust to details in the 'red galaxy' definition.

Fig. 8 also shows that Tanaka et al. (2005) V band LF. It is ≈ 0.75 mag too bright, for reasons that we are unable to understand.

Overall, our LF is in agreement with previous works. It is deeper and has smaller errors than previously published LFs and, thanks to the rigorous analysis, it is considered more reliable.

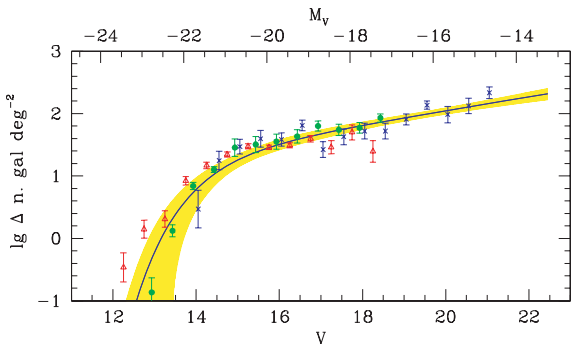

Figure 8. V-band LF of red galaxies in Abell 1185 (shaded region), Coma (Secker & Harris 1996; blue crosses), two $z = 0.2$ clusters (Smail et al. 1998; green points), and nearby clusters in Tanaka et al. (2005; red triangles). All LFs are normalized (vertically shifted) to Abell 1185 down to $M_V = 18$ mag. All LFs, except Tanaka et al. (2005), agree with each other. Abell 1185 goes deeper than the other LFs and has smaller errors.

4.3 A more complex LF of red galaxies?

In this section, we ask ourselves if our LF model should be updated with regard to the published LFs, i.e. if the red galaxy LF is cluster-dependent: in particular, whether we should use a more complex LF in order to account for the possible existence of a dip, i.e. a region with depressed counts, a feature actively debated in the literature (e.g. Biviano et al. 1995; Secker & Harris 1996).

We found no evidence for a dip in Abell 1185 (see Fig. 6) and therefore we looked with further attention to the published claims about its existence. We consider with special attention Secker & Harris (1996), because the authors excel in accounting for the uncertainty in the background subtraction and in providing all the statistical details needed to reanalyse their data. They find that the LF of red galaxies in the Coma cluster is well modelled by a sum of a Gaussian and a Schechter, suggested by the presence of a possible dip in the Coma LF at $M_R \sim -19$ mag.

The simple Schechter model that best-fitting Abell 1185 data are a good description of their data (of Coma) and the $\chi^2 = 22$ for 15 degrees of freedom (i.e. larger χ^2 are observed 10 per cent of the time under the null hypothesis that the data are drawn from the model), as can also qualitatively be seen in Fig. 8. This comparison suggests that, in light of our results on Abell 1185 (which were of course not available at the time of their analysis), their data do not *require* a model more complex than a Schechter with α and M^* fixed to the best-fitting Abell 1185 values. The Bayesian Information Criteria (Schwarz 1978; Liddle 2004, provides a useful astronomical introduction) quantitatively inform us that evidence is largely in favour of the simplest model.

We cannot repeat the above analysis with other published works because they usually do not provide all the necessary details. Qualitatively, a model with a dip seems unnecessary, even when the p value of the data (computed using χ^2 or another statistic) is small (i.e. the fit with a Schecther function is claimed to be bad), because the increase in the log-likelihood obtained by introducing the extra parameters is more than compensated by the huge increase in dimensionality of the parameter space over which the likelihood should be averaged.

4.4 Discussion on methods

4.4.1 Impact of the method used

Compared to previously published works, the CM presented in this study has been determined in a fairly different way and therefore it is important to discuss whether our results may depend or not on the analysis method. We derived all our results twice: first using the common method currently used in literature, and then using a statistical method based on axioms of probabilities. The two methods give the same results qualitatively but the second method has the advantage of providing results with guaranteed correctness, as opposed to a blind application of basic rules potentially giving misleading results, as detailed also in APG, Andreon et al. (2006), and also by several previous works (e.g. Kraft et al. 1991; Loredo 1992).

The most notable difference between our study and the previous works is that, instead of subtracting the background of galaxies, we account for it more rigorously. The present work is a continuation of activities started in APG, and continued in Andreon et al. (2006) and Andreon (2006).

The usual astronomical recipe for background subtraction, $n_{\rm clus} = n_{\rm tot} - n_{\rm bkg}$, called the unbiased estimator by sampling theories (e.g. MacKay 2005), has a somewhat different meaning from what

it seems. Let us suppose, for example, that three galaxies are observed in the cluster line of sight and five are expected given our (assumed to be quite precise) control field observations. This situation is possible, because of Poisson fluctuations. If we compute the cluster contribution as the difference between the above two numbers, we find a negative number of galaxies in the cluster (or say in a given location of the parameter space, i.e. in a given range of colours and magnitude), leading to the unphysical result of non-positive numbers of galaxies. Therefore, $n_{\rm tot} - n_{\rm bkg}$ is an estimator of $n_{\rm clus}$ that in certain conditions has properties that are not acceptable.

A naive solution to avoid unphysical values is to set these negative values to zero. However, this correction overestimates the total number of cluster galaxies (i.e. the one of the whole sample), because negative fluctuations have been corrected all in the same direction by increasing them and positive fluctuations have been left untouched (effectively a Malmquist-type bias). Another possible naive solution is to widen the bin size (if data are binned), until unphysical values disappear. Physically, it may happen that the bin becomes much larger in a direction than the uncertainty of the data points it contains. In such a situation, in order to remove an unphysical result, we are forced first to put in the same bin incompatible data (because they are several σ away from each other) and then to subtract off each other incompatible data, a procedure that can only lead to doubtful results. This situation often occurs at the less populated bright magnitudes, where errors are small.

Therefore, if $n_{\rm tot} - n_{\rm bkg} < 0$, we are in an unsatisfactory position: we may choose between (i) having unphysical values at some location and an unbiased total number count, or (ii) having physical values for individual measurements and a biased value for the whole sample, or (iii) adding/subtracting incompatible data points from each other. Actually, the same problem holds for $n_{\rm tot} - n_{\rm bkg} \gtrsim 0$ (of which some aspects are called the Malmquist bias in literature, see Jeffreys 1938 for a lucid discussion), and has already been discussed in Kraft et al. (1991), APG and Andreon et al. (2006) and others. As soon as the dimensionality of the data space is large, or when, as in the present case, the distribution of the data in the data space are uneven, there will always be some bins/location where $n_{\rm tot} - n_{\rm bkg} \approx 0$, i.e where some problems arise.

The second shortcoming of the usual astronomical recipe, $n_{\rm tot} - n_{\rm bkg}$, concerns the measurement of its uncertainty. When the difference above is negative, a valid confidence interval (at whatever confidence level) is an empty interval (Kraft et al. 1991). With the confidence interval empty, no interval can be shorter, not even the one derived in the absence of any background, which is an incoherent result. For example, contrary to common sense, one may conclude because of that approach that it makes no sense to perform a redshift survey to determine the individual membership of every galaxy in the sample, because these new observations will lead to larger confidence intervals! The null length of the confidence interval produces another absurd result. Let us suppose that the derived confidence interval turns out to be of positive length. There is an easy way to make it smaller: by *adding* a background in the hope that Poisson fluctuations make $n_{\rm tot} - n_{\rm bkg} < 0$. For a sufficiently large background, the above occurs 50 per cent of the time. Such a solution, although formally correct, is unacceptable intuitively because it implies adding noise in order to reduce uncertainties!

The third shortcoming of the usual astronomical recipe comes from binning the data. As discussed in APG, seldom are the size, number and location of bins considered, as well as their relevance for the final results. Has a trend been missed because of the non-optimal quantization of data in bins?

Bayesian methods do not present such troubles, because of the following.

(i) They do not require that data are binned.

(ii) They are squarely based on axioms of probabilities (i.e. returning credible intervals in agreement with logic and common sense). Specifically, instead of removing the background, we introduced the background component and we then marginalized the posterior over the nuisance (background) parameters, as required by the sum axiom of probability.

(iii) They naturally account for boundaries in the data or parameter space. In the present work, several parameters have boundaries: for example, the intrinsic scatter of the CM relation and the number of cluster or field galaxies cannot be negative.

Therefore, for display purposes we use astronomical recipes, which often hold, but adopt a full Bayesian computation for estimating parameters (and uncertainties) and for model selection. The appendix of Andreon (2006) describes in detail the stochastical computation using the Monte Carlo Marcov Chain (MCMC, Metropolis et al. 1953) method used to determine the CM relation.

The full Bayesian computation and the use of common rules both provide compatible results: in fact, in all figures showing data points computed with astronomical recipes, and models computed with probability axioms, the two derivations agree each other. For example, curves and data points in Fig. 6 agree with each other. The CM slope derived from the theory of probabilities (solid line in Fig. 2) agrees with data points in Fig. 2. The full Bayesian computation is however not useless. The agreement between the two approaches has been 'guided' by the more precise computation: for example, in Fig. 6, by taking much smaller bins, we easily get negative numbers of cluster galaxies and also an unbelievable LF that takes only discrete values (because cluster galaxies come in integer units), which is an unphysical result. Furthermore, 'guided' by the Bayesian analysis, in Fig. 6 we did not plot confidence intervals (that have the mentioned shortcoming of not becoming small when the uncertainty on nuisance parameters decreases and of potentially being of null length), but we computed the (approximated) variance of the estimator $n_{\rm tot} - n_{\rm bkg}$. One of the advantages of Bayesian methods is that they *always* return numbers with guaranteed correctness; the disadvantage is that sometime they are expensive to implement computationally.

The LF is determined strictly following APG, i.e. a maximum likelihood method, to which we defer for details, instead of a determination from a fully Bayesian derivation. In the present paper, we took advantage from the fact that regularity conditions for the use of the likelihood ratio theorem hold for LF computations and therefore we used the inexpensive maximum likelihood method instead of the CPU-expensive Bayesian approach for the stochastical computations.

4.4.2 The role of assumptions

During our CM determination in the Appendix, we made several assumptions.

First of all, we determined the slope of the CM assuming its linearity. However, if the CM is bent, the meaning of 'slope' (a number, indeed) is ill-defined: i.e. what is the slope of a bent line? Therefore, a valid question that precedes the slope determination is: is the CM bent or linear? The task of choosing a model from

a set of potential models is called model selection, and we encountered it when discussing this very same issue for Virgo galaxies (Section 4.1) and again when we commented about the existence of a dip in the LF (Section 4.2). As done in Section 4.1, to answer the question, it is just matter of increasing the degree of the polynomial describing the CM relation shape and comparing the relative evidence of the two models: the linear model turns out to be highly preferred. The outcome of this comparison is quite expected, the CM is clearly linear, as the inspection of Fig. 4 at bright magnitudes clearly demonstrates, as well as Fig. 3 at faint magnitudes, and Fig. 5 over the whole magnitude range. The first two plots are two simple projections of the data cube, for which no analysis whatsoever has been applied. In Fig. 5, instead, the background has been removed, by quantizing data in bins in the colour–colour–magnitude plane.

Secondly, we further assumed that the LF of red galaxies is described by a Schechter function and that the distribution of background galaxies can be modelled as a polynomial in the restricted range of colours we are interested in. The former assumption is justified by Fig. 6 (see the data points, derived without any assumption about the LF shape). The latter assumption is quite general: every distribution sufficiently smooth can be approximated by its Taylor expansion, which is a polynomial. Therefore, we raised the degree of the polynomial until a satisfactory match with the data was reached.

4.4.3 Conclusions on methods

The performed analysis squarely relies on laws of probabilities and accounts for the existence of boundaries. Of course, it is possible to follow a simpler path to derive the results, but we cannot guarantee the correctness of the results obtained by methods that ignore (or do not fully account for) laws of probabilities and the existence of boundaries in the data or parameter space.

4.5 Discussion of results

The CM relation has a simple interpretation in the context of galaxy formation: the brighter and more massive galaxies have deeper gravitational potential wells and therefore are more prone at retaining the interstellar gas, which becomes superheated and metal enriched during the initial stages of the star formation epoch (Dekel & Silk 1986). Assuming that the magnitude blueing of the red sequence is only due to metallicity and adopting the Harris (1996) [Fe/H] versus $B - R$ calibration, galaxy metallicity changes by 1.2 dex in the explored magnitude range. Although the CM sequence is interpreted in terms of a metallicity trend (Kodama & Arimoto 1997), our data alone may be interpreted in terms of age (fainter galaxies are younger and thus bluer), because of the well-known age/metallicity degeneracy (e.g. Worthey 1994).

Abell 1185 does not present the appealing features claimed to have been observed in other clusters and discussed at length in previous published works. Its red sequence does not disappear at faint magnitudes and neither bends towards red or blue colours: it simply continues straight, following the extrapolation of what is usually observed at brighter magnitudes. The scatter along the CM does not largely increase with magnitude as claimed for galaxies in the Perseus clusters. The LF of red galaxies shows no dip and no passband dependence.

All the above points offer us the chance of not looking for physical mechanisms affecting the features of the objects in such a way as to produce the (unobserved) heterogeneity. The absence of features points towards a homogeneity of red galaxies over the whole 9-mag range explored (four decades in stellar mass). Our argument is the usual one and can be found in most papers discussing the homogeneity of red galaxies (e.g. Bower et al. 1992; Andreon 2003), with the only difference being that what is discussed for bright galaxies holds here for the extreme faint galaxies: homogeneity in colour implies an old star age or a synchronization between the history of star formation of the various galaxies.

Faint ($M \approx M^* + 3$ mag) red galaxies have attracted the attention of astronomers in recent days. At high redshift, the CM relation sees signs of depletions: i.e. it has been reported that, at $M^* + 2.5$, the CM relation disappears (Kodama et al. 2004) or it is strongly underpopulated (De Lucia et al. 2004). On the other end, the effect does not appear to be universal, because the $z = 0.83$ MS 1054 cluster does not show any signs of depletion (Andreon 2006) down to $M^* + 3.5$ mag. We defer to Andreon (2006) for a detailed discussion about the reality of the claimed deficit of faint red galaxies. Kodama et al. (2004) and De Lucia et al. (2004) conclude that faint ($M^* + 3$) red galaxies are a recent ($z \lesssim 1$) population. This interpretation does not fit our data: if faint red galaxies are younger than brighter red galaxies, then they should not lay on the extrapolation at faint magnitudes of the CM relation observed at brighter magnitudes (i.e. the CM should bend towards the blue) and the scatter should increase towards faint magnitudes (there is less time for the objects to make their colour more similar). Quantification of the offset to be observed is simple: if faint galaxies form at $z \sim 0.8$ instead of $z \sim 3$, they should be bluer by 0.06 mag in $B - V$ (assuming a single stellar population, e.g. Buzzoni 2005), a drift that we do not see in Abell 1185.

5 CONCLUSIONS

We have studied the colour of red galaxies of the Abell 1185 cluster at $z = 0.0325$ down to $M^* + 8$ in the B, V and R bands. The CM relation is linear without evidence for significant bending down to absolute magnitudes seldom probed in literature ($M_R = -12.5$ mag). It is also thin (± 0.04 mag) and its thickness is not a strong function of magnitude. The LF of red galaxies in Abell 1185 is adequately described by a Schechter function, with a characteristic magnitude and faint end slope that also well describe the LF of red galaxies in other clusters. There is no passband dependence of the LF shape, other than an obvious M^* shift due to the colour of the considered population. Red galaxies form a homogeneous population, over four decades in stellar mass, for what concerns colours and luminosity. Homogeneity in colour implies an old star age or a synchronization between the history of star formation of the various galaxies, down to $M^* + 8$.

ACKNOWLEDGMENTS

SA thanks Giancarlo Ghirlanda and Giovanni Punzi for useful discussion of the 68 per cent confidence bounds and Masayuki Tanaka for giving us his and his colleagues' red LF in electronic form. J-CC thanks Gregory Fahlman for giving us discretionary time to realize this project.

Based on observations obtained at the CFHT, which is operated by the National Research Council of Canada, the Institut National des Sciences de l'Univers of the Centre National de la Recherche Scientifique of France, and the University of Hawaii.

Other facilities used (to which we defer for standard acknowledgements) include the NASA/IPAC Extragalactic Database (NED).

REFERENCES

Abell G. O., 1958, ApJS, 3, 211
Andreon S., 2003, A&A, 409, 37
Andreon S., 2006, MNRAS, 369, 969
Andreon S., Cuillandre J.-C., 2002, ApJ, 569, 144 (AC02)
Andreon S., Lobo C., Iovino A., 2004, MNRAS, 349, 889
Andreon S., Punzi G., Grado A., 2005, MNRAS, 360, 727 (APG)
Andreon S., Quintana H., Tajer M., Galaz G., Surdej J., 2006, MNRAS, 365, 915
Bertin E., Arnouts S., 1996, A&AS, 117, 393
Biviano A., Durret F., Gerbal D., Le Fevre O., Lobo C., Mazure A., Slezak E., 1995, A&A, 297, 610
Blanton M. R., Lupton R. H., Schlegel D. J., Strauss M. A., Brinkmann J., Fukugita M., Loveday J., 2005, ApJ, 631, 208
Bower R. G., Lucey J. R., Ellis R. S., 1992, MNRAS, 254, 601
Bruzual A. G., Charlot S., 1993, ApJ, 405, 538
Buzzoni A., 2005, MNRAS, 361, 725
Conselice C. J., Gallagher J. S., Wyse R. F. G., 2002, AJ, 123, 2246
Cuillandre J.-C., Luppino G., Starr B., Isani S., 2000, SPIE, 4008, 1010
D'Agostini G., 2003, Bayesian reasoning in data analysis - A critical introduction. World Scientific Publishing, River Edge
D'Agostini G., 2005, online only reference: http://arxiv.org/abs/physics/0511182
Dekel A., Silk J., 1986, ApJ, 303, 39
De Lucia G. et al., 2004, ApJ, 610, L77
Drinkwater M. J., Phillipps S., Gregg M. D., Parker Q. A., Smith R. M., Davies J. I., Jones J. B., Sadler E. M., 1999, ApJ, 511, L97
Evans R., Davies J. I., Phillipps S., 1990, MNRAS, 245, 164
Ferrarese L. et al., 2006, ApJS, 164, 334
Garilli B., Maccagni D., Andreon S., 1999, A&A, 342, 408
Harris W. E., 1996, AJ, 112, 1487
Jeffreys H., 1938, MNRAS, 98, 190
Jones C., Forman W., 1984, ApJ, 276, 38
Kodama T., Arimoto N., 1997, A&A, 320, 41
Kodama T. et al., 2004, MNRAS, 350, 1005
Kraft R. P., Burrows D. N., Nousek J. A., 1991, ApJ, 374, 344
Landolt A. U., 1992, AJ, 104, 340
Liddle A. R., 2004, MNRAS, 351, L49
Loredo T., 1992, in Feigelson E. D., Babu G. J., eds, Statistical Challenges in Modern Astronomy. Springer-Verlag, New York, p. 275
McCracken H. J. et al., 2003, A&A, 410, 17
MacKay D., 2005, Information theory, Inference and Learning Algorithms. Cambridge Univ. Press, Cambridge
Magnier E. A., Cuillandre J.-C., 2004, PASP, 116, 449
Mahdavi A., Geller M. J., Fabricant D. G., Kurtz M. J., Postman M., McLean B., 1996, AJ, 111, 64
Mateo M. L., 1998, ARA&A, 36, 435
Metropolis N., Rosenbluth A., Rosenbluth M., Teller A., Teller E., 1953, J. Chem. Phys., 21, 1087
Oemler A. J., 1974, ApJ, 194, 1
Sandage A., Tammann G. A., Yahil A., 1979, ApJ, 232, 352 (STY)
Schechter P., 1976, ApJ, 203, 297
Schwarz G., 1978, Ann. Stat., 5, 461
Secker J., Harris W. E., 1996, ApJ, 469, 623
Secker J., Harris W. E., Plummer J. D., 1997, PASP, 109, 1377
Smail I., Edge A. C., Ellis R. S., Blandford R. D., 1998, MNRAS, 293, 124
Tanaka M., Kodama T., Arimoto N., Okamura S., Umetsu K., Shimasaku K., Tanaka I., Yamada T., 2005, MNRAS, 362, 268
Trotta R., 2005, online only reference: http://theory.physics.unige.ch/~trotta/html/software.htm
Visvanathan N., Sandage A., 1977, ApJ, 216, 214
Wilks S., 1938, Ann. Math. Stat., 9, 60
Wilks S., 1963, Mathematical Statistics. Princeton Univ. Press Princeton
Worthey G., 1994, ApJS, 95, 107
Zwicky F., 1957, Morphological Astronomy. Springer, Berlin

APPENDIX A: TECHNICAL DETAILS

In Section 3, we do not provide quantitative details about the way the slope and scatter of the CM relation of cluster galaxies have been determined, a gap that we fill in this Appendix. We strictly follow Andreon (2006) who presents the statistical approach, starting from axioms of probability and largely following D'Agostini (2003, 2005). In short, we model the cluster distribution in the CM plane as the product of a Schechter function in magnitude and a linear CM relation with an intrinsic unknown scatter. Furthermore, we model the background distribution in the CM plane as the product of a power law of degree two in magnitude and of degree one in colour times a Gaussian in colour with unknown dispersion whose central colour is linear depending on magnitude with an unknown slope and intercept. Such a modelling requires seven nuisance parameters for the background, over which we marginalize in order to derive the uncertainty on the interesting quantities (e.g. the parameters describing the CM relation). The wide magnitude range and the abundant background data considered in this paper both oblige us to adopt a model with many parameters for the background; however, such a complicated model is still insufficient to describe the background distribution over the whole magnitude range accessible to the observations. Therefore, instead of increasing the model complexity of the background (which encodes information that is not of interest to us in this paper), we prefer to discard the last magnitude bin, where the background contribution is so large that it carries very poor information about the slope and intercept of the CM relation (i.e. in our CM determination, we use $R < 21$ instead of $R < 22$).

One of the merits of this approach is that it does not claim that it is plausible that the scatter around the CM is negative, whereas other methods claim that negative (and therefore unphysical) values of the scatter are within the 68 per cent confidence interval.

As in Andreon (2006), we are not interested in modelling the distribution of red galaxies at colours where they are not observed, and therefore we limit the analysis to the $0.4 < V - R < 0.9$ mag and $0.7 < B - V < 1.5$ mag ranges. Assuming uniform priors zeroed in the unphysical ranges, we found:

$$B - V = 0.986 \pm 0.007 - (0.038 \pm 0.003)(R - 19.556) \text{ mag}$$

with a scatter of 0.039 mag and

$$V - R = 0.608 \pm 0.007 - (0.016 \pm 0.002)(R - 19.556) \text{ mag}$$

with a scatter of 0.036 mag.

This paper has been typeset from a TEX/LATEX file prepared by the author.